Development and Validation of a High-Vacuum Thermal Conductivity Testbed for Aerospace Interface Materials

Amy Chang (NASA MSFC), Debby Hernandez (Amentum SED)

Presented By
Amy Chang

Thermal & Fluids Analysis Workshop
TFAWS 2026
August 31 – September 4, 2026
NASA Marshall Space Flight Center
Huntsville, AL

Outline

- Motivation
- Calibration Test Article
- Thermal Model
- Multilayer Material Test Article
- Results
- Future Work

Motivation: Thermal Conductivity in Space Systems

- Spacecraft thermal-control systems often rely on a sequence of conductive interfaces between a heat-generating component and a final heat sink.
- In vacuum, natural convection and gas-phase conduction are negligible; therefore, component temperatures are governed primarily by solid conduction through mechanical interfaces with surrounding surfaces.

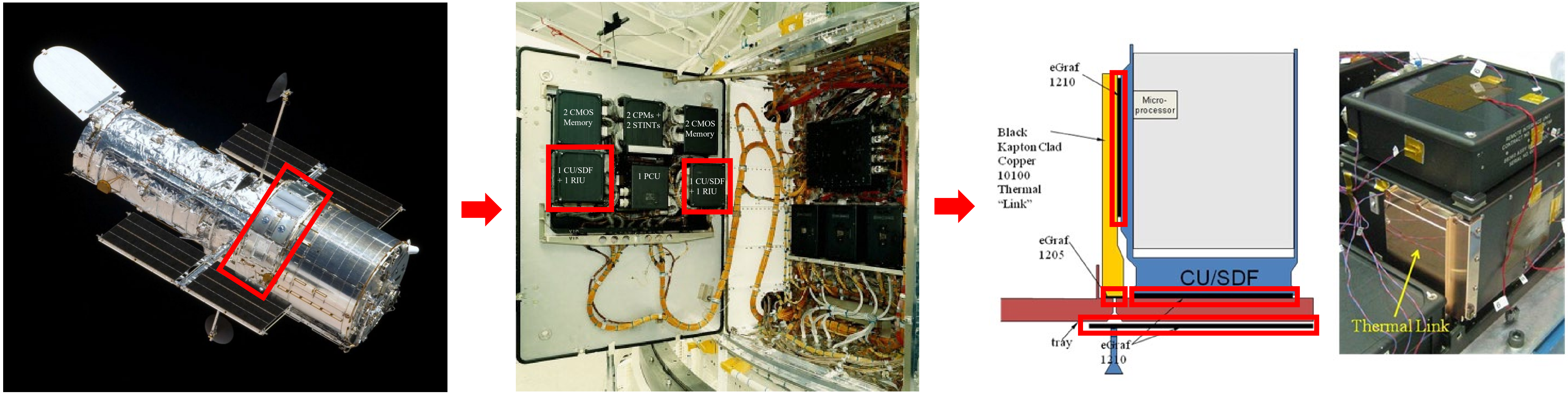

Figure 1. Hubble Space Telescope Science Instrument Control and Data Handler 2 thermal link design and implementation.

[1] T. Gregory, J. Abel and J. Mandi, "Thermal Design Considerations of the Hubble Space Telescope (HST) Science Instrument Control and Data Handler (SI C&DH-2)," in 40th International Conference on Environmental Systems, Barcelona, 2012.
[2] European Space Agency, "Science Instrument Control and Data Handling Unit," 30 September 2008. [Online]. Available: https://sci.esa.int/s/8r0XPkw. [Accessed 2026].

Experimental Overview

To address this, a modular ambient/vacuum testbed was developed and evaluated to measure installed thermal performance and extract model-conditioned estimates of thermal conductivity and contact resistance for thermal interface materials.

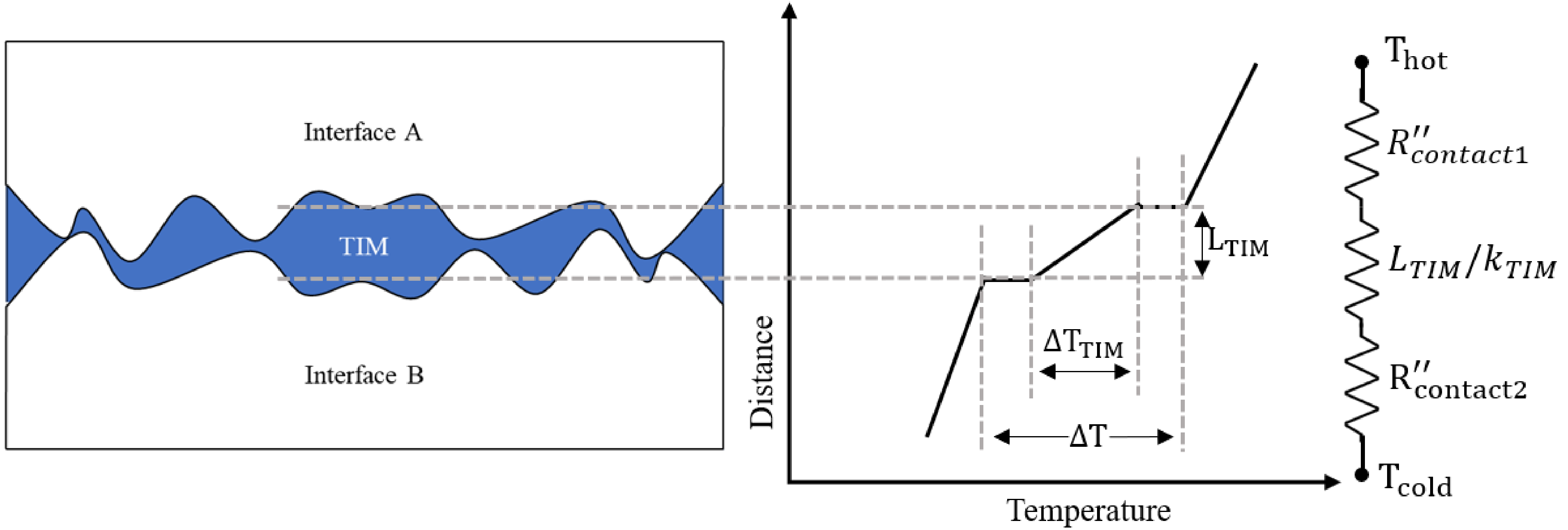

$$R''_{joint} = R''_{contact,1} + \frac{L_{TIM}}{k_{TIM}} + R''_{contact,2} = \frac{L_{TIM}}{k_{app}}$$

Test Article

FRONT VIEW:

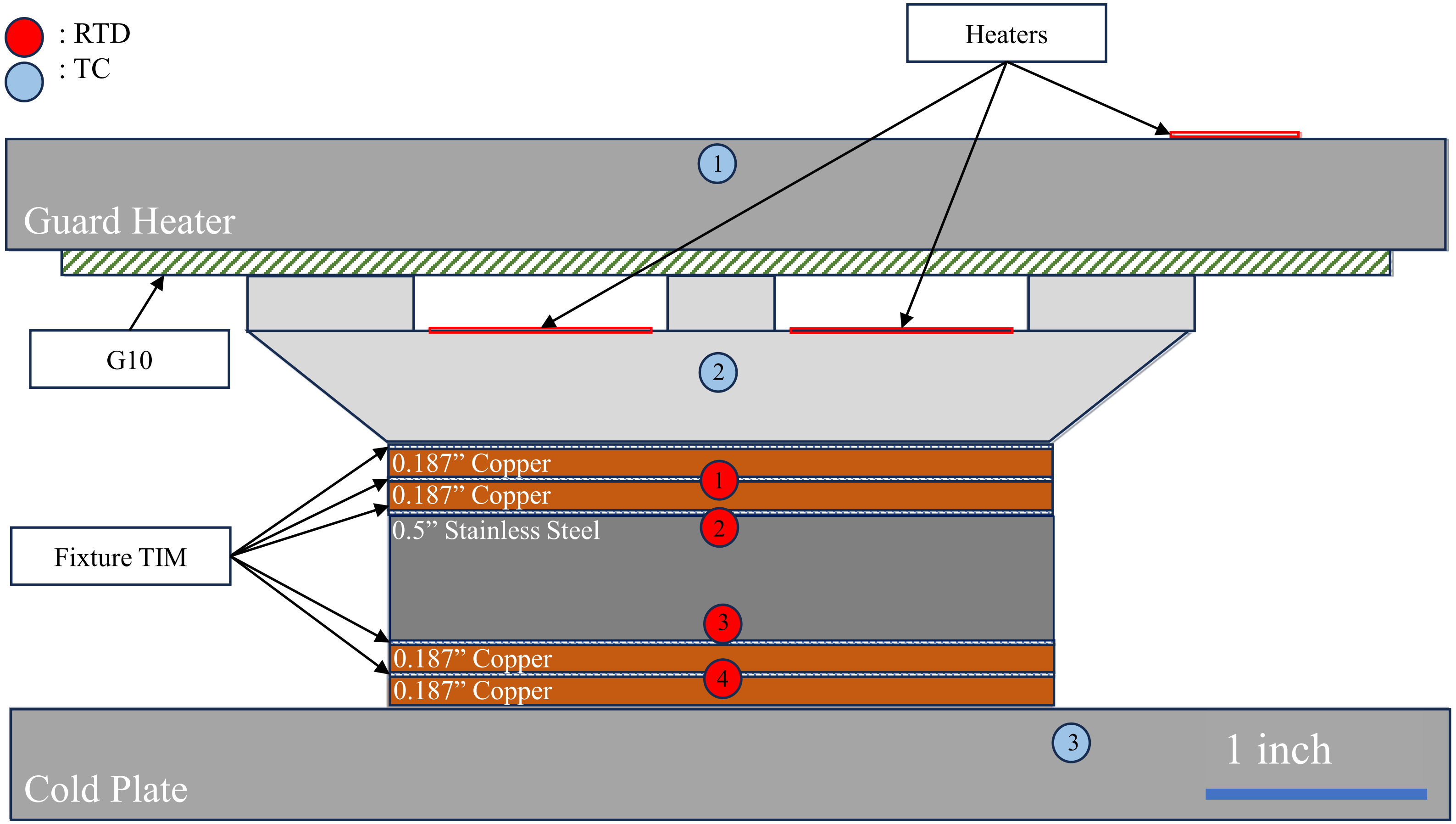

Test Stack

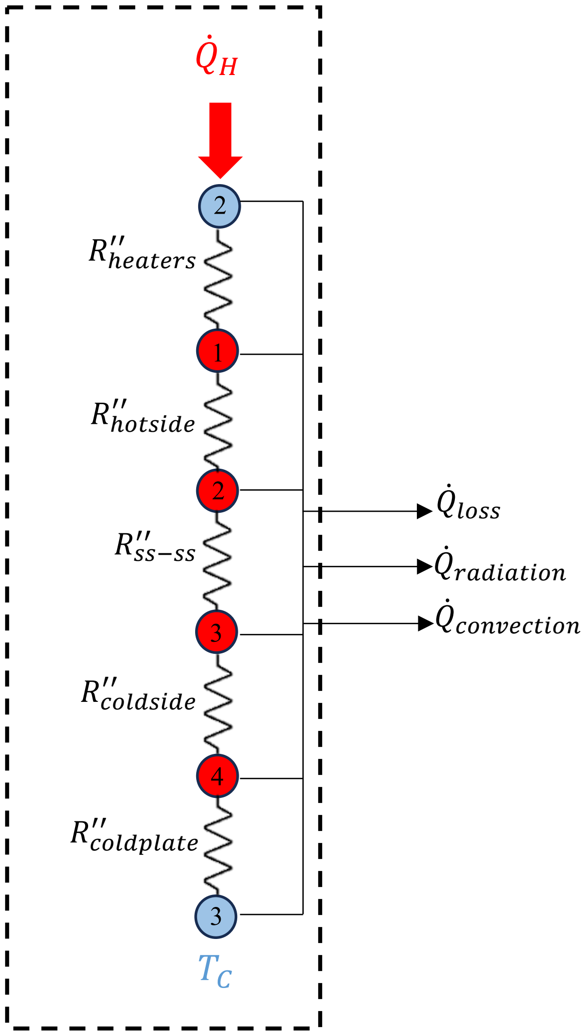

Notes:

- RTD1 and RTD4 are embedded in between the copper plates.
- TC1 was secure on the top of the guard heater.
- TC4 was secured between the MLI and the stack.
- TC5 was secured 1 inch off the vacuum chamber ceiling.
- Fixture TIM is Braycote 601EF in all presented cases.

Sensor and MLI Placement

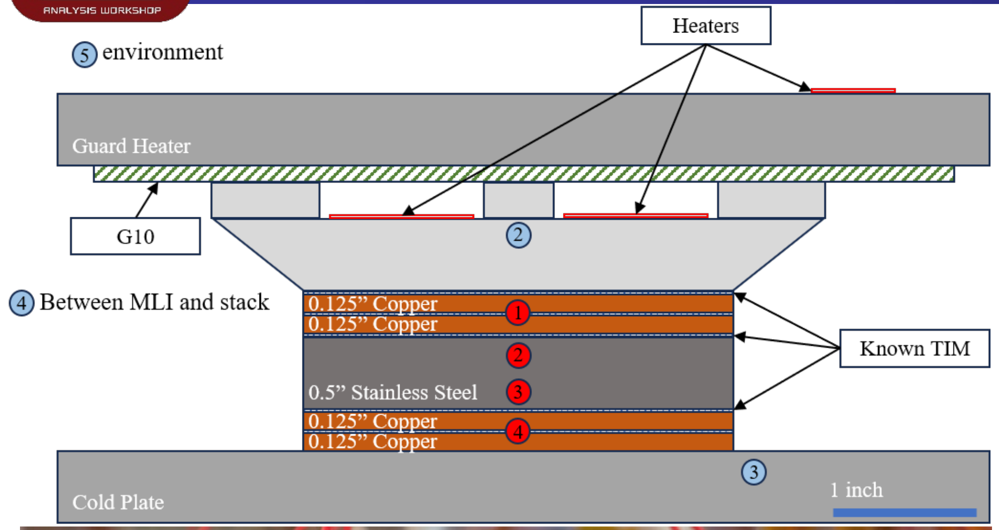

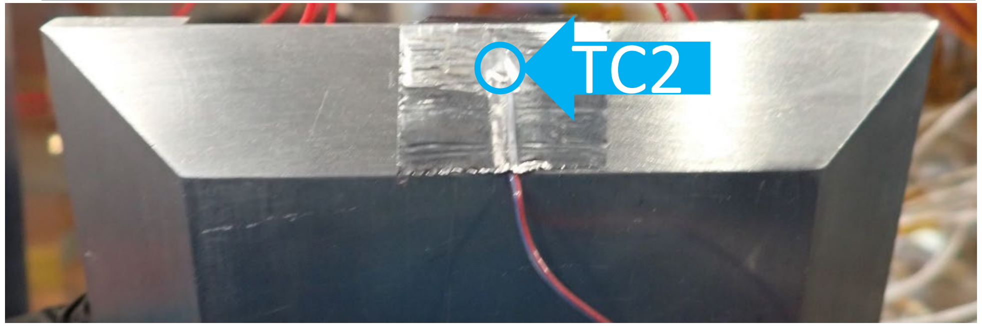

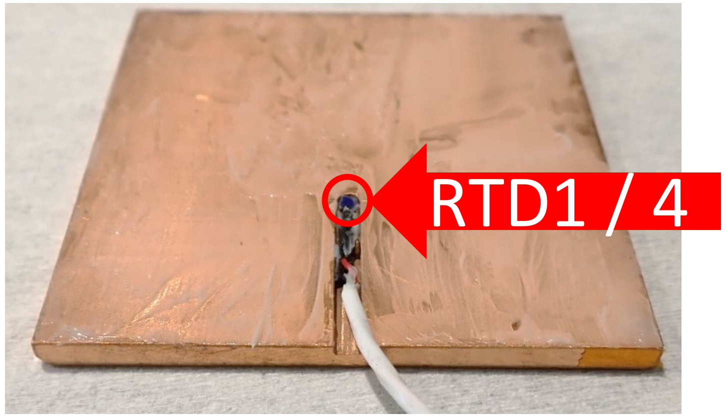

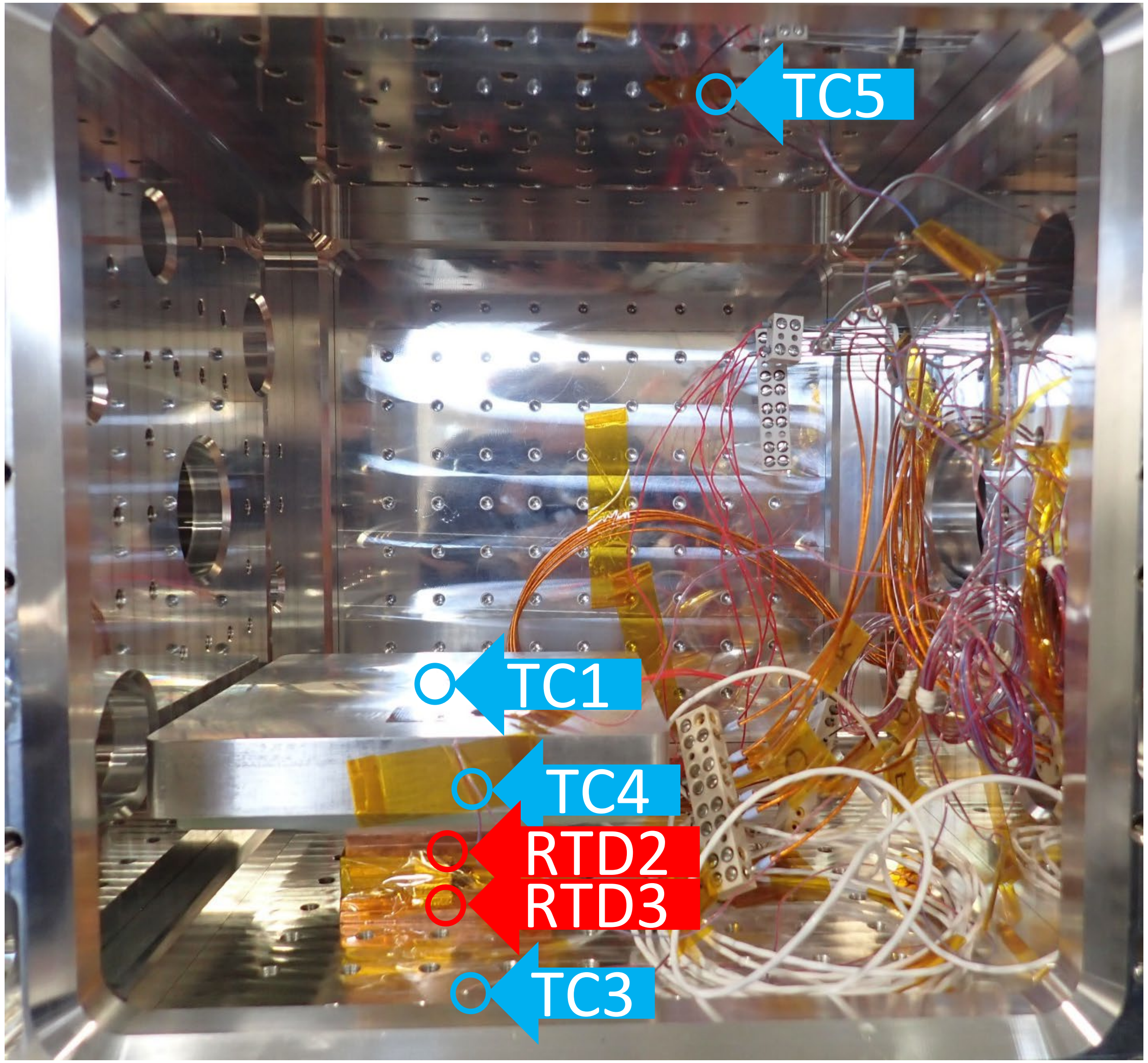

MLI Placement

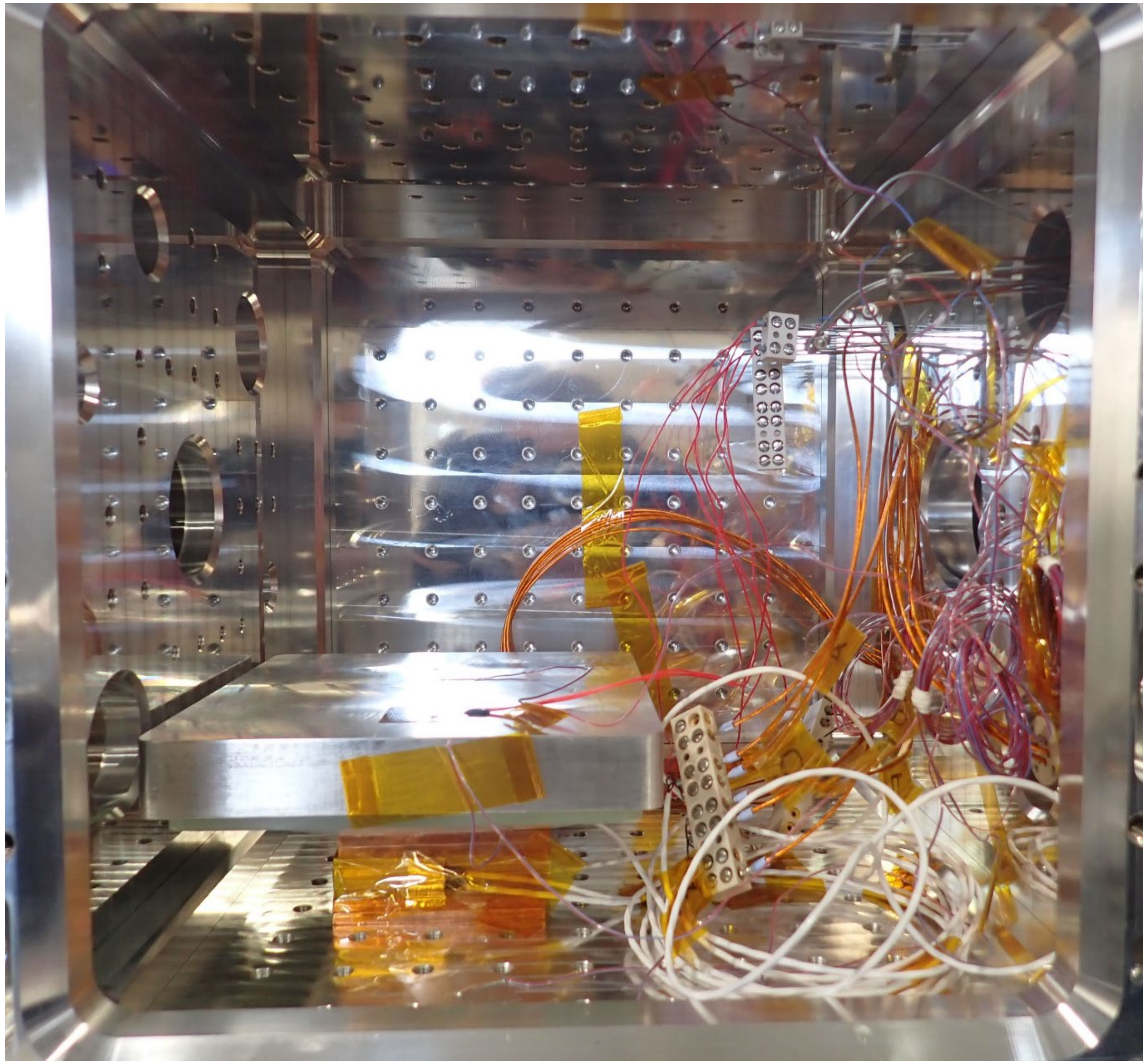

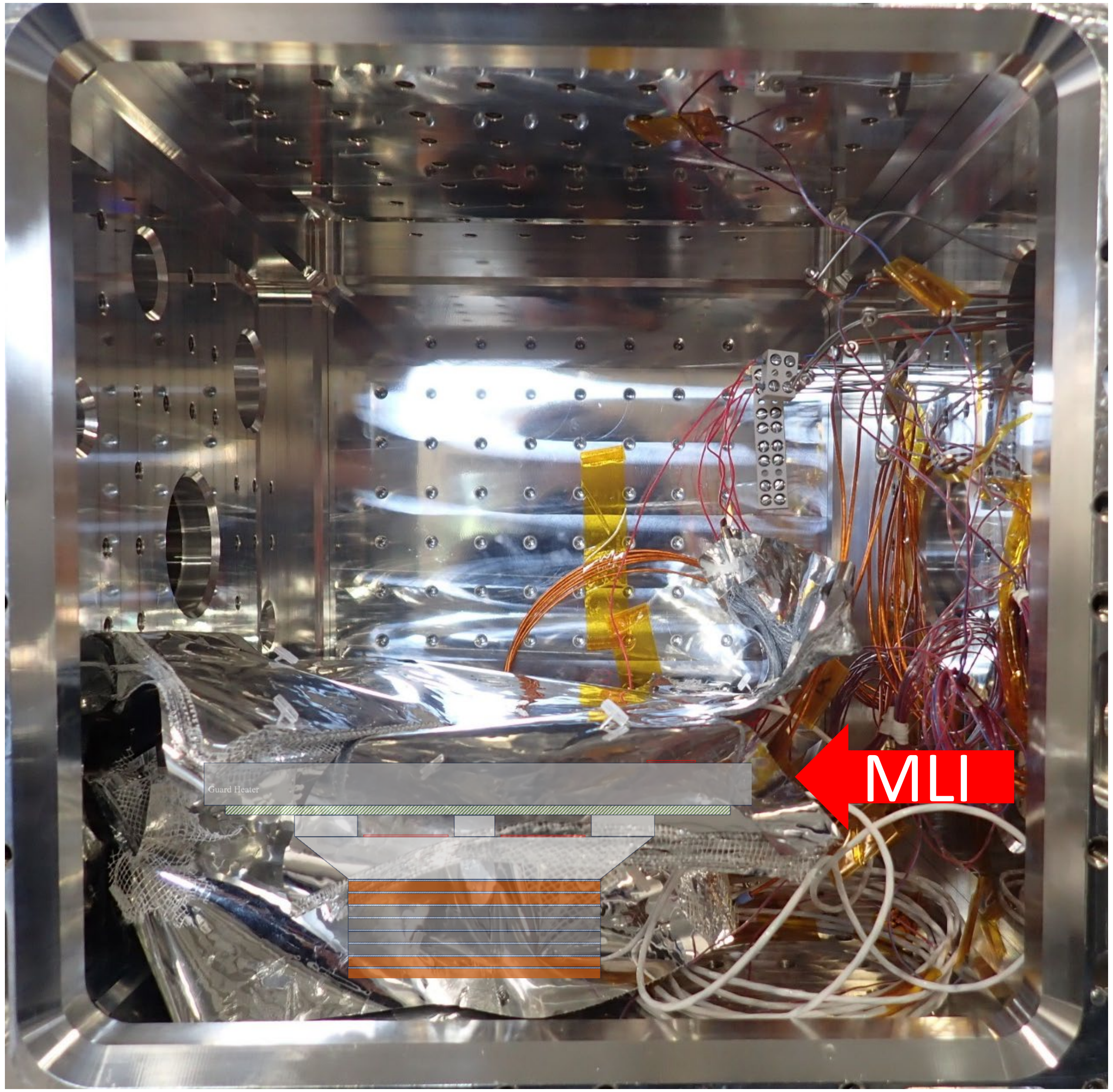

Test Equipment

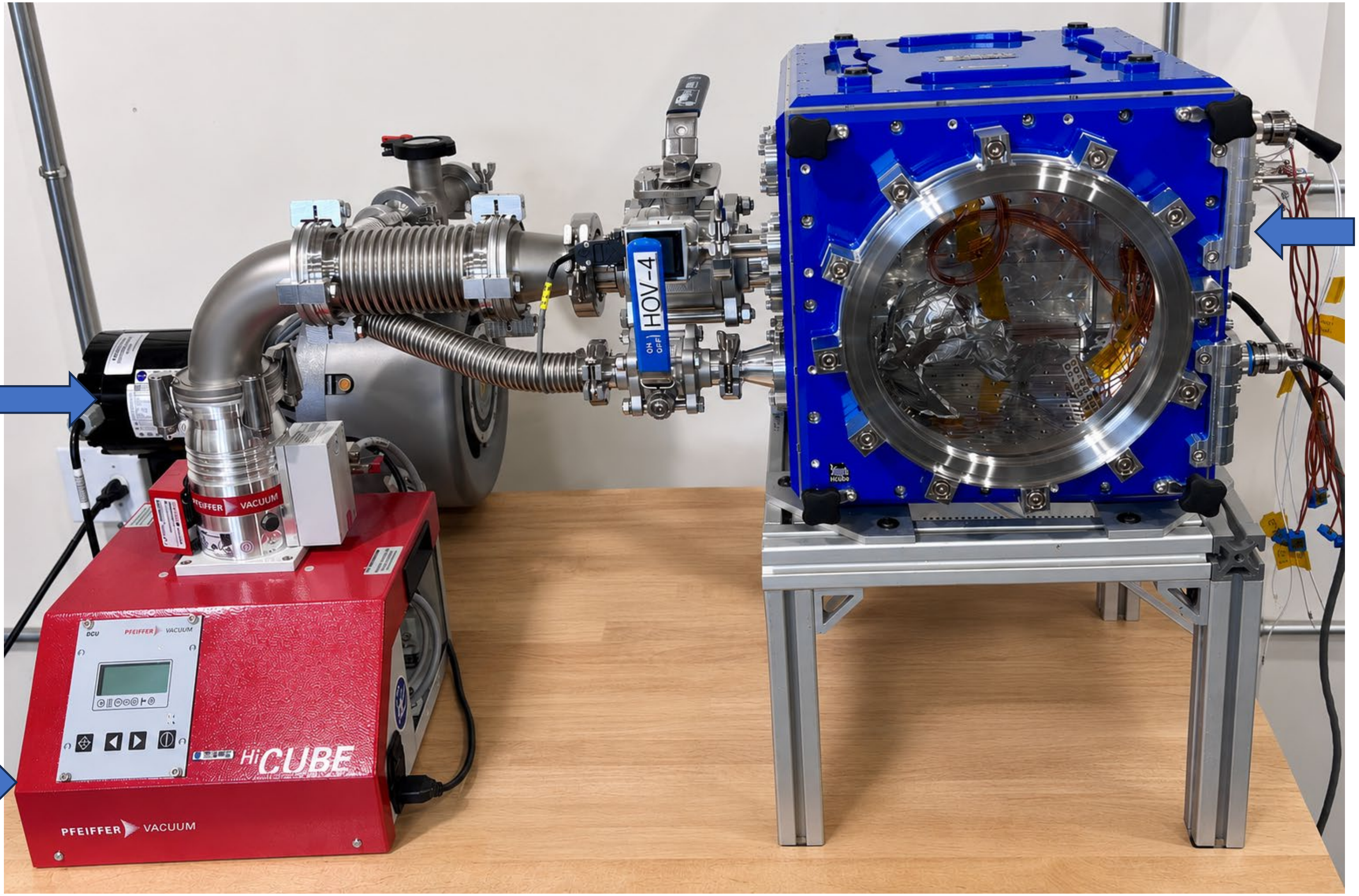

Roughing Pump

Turbo Pump

12 in x 12 in x 12 in Vacuum Chamber

Thermal Network

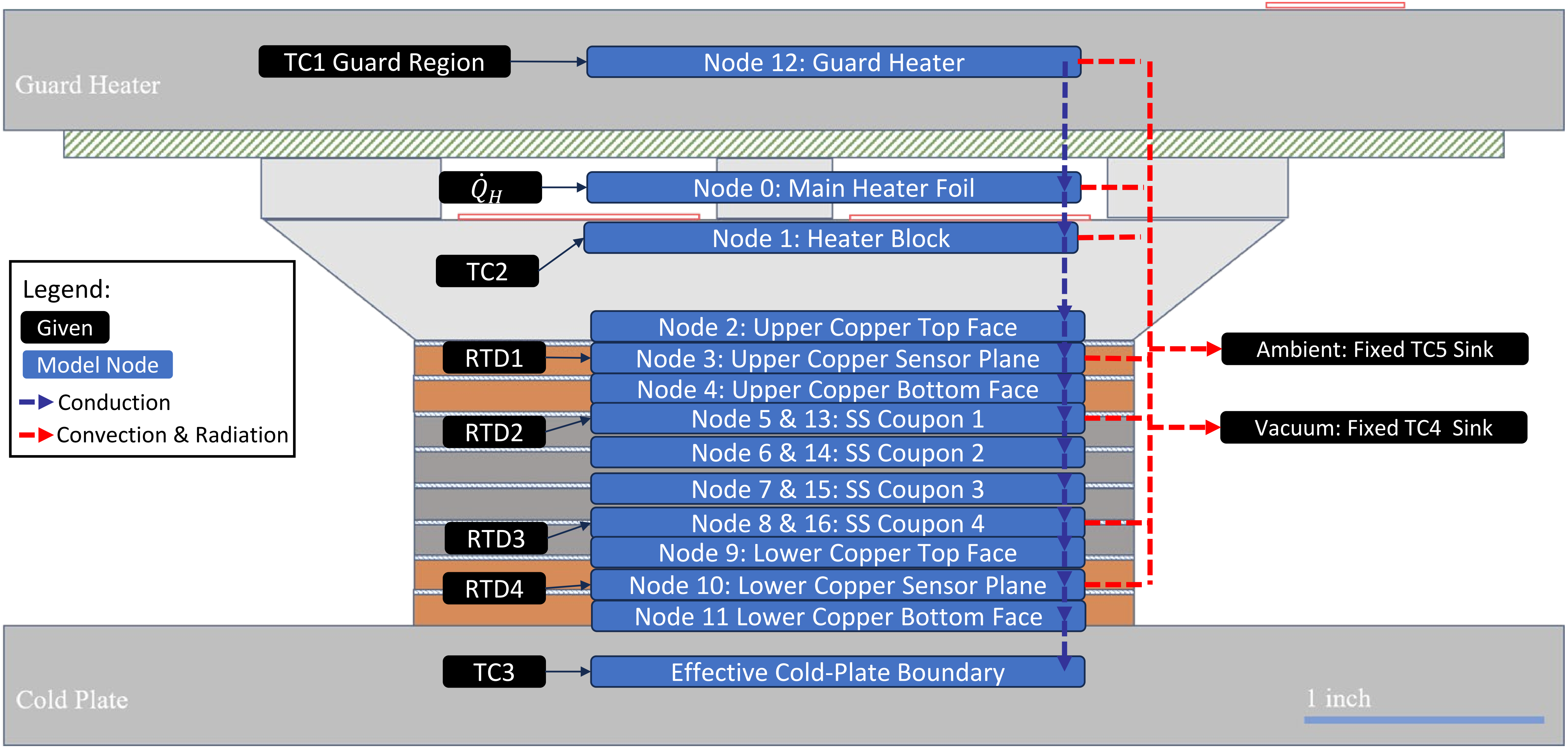

Model Assumptions and Inputs

$$\dot{Q}_{conduction} = \frac{kA}{L}(T_i - T_j)$$
$$\dot{Q}_{convection} = hA(T_i - T_\infty)$$
$$\dot{Q}_{radiation} = \varepsilon\sigma A(T_s + T_{sur})(T_s^2 + T_{sur}^2)(T_s - T_{sur})$$

TAIMV Calibration, Transfer, and Extraction Logic

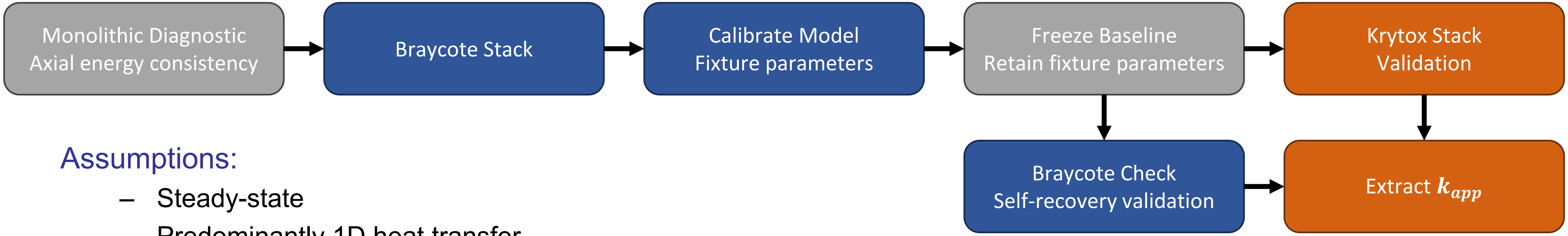

Assumptions:

- Steady-state
- Predominantly 1D heat transfer
- Constant test article material properties
- Radiation is linearized
- Vacuum cases neglect gas conduction and convection
- Contact resistances and fixture parasitic losses are transferred from calibration
- Only gravity-driven compression is represented

Inputs:

- Test configuration
- Hot and cold boundary conditions
- Boundary Temperatures (TC 1-5)
- Stack Temperatures (RTD 1-4)
- TIM properties (ex: $L_{TIM}, k_{TIM}, \rho_{TIM}$)

Heat Flow Partitioning Requires Model-Based Reduction

$$P_{main} = \dot{Q}_{stack} + \dot{Q}_{radiation} + \dot{Q}_{convection} + \dot{Q}_{guard} + \dot{Q}_{residual} = \dot{Q}_{stack} + \dot{Q}_{nonstack}$$

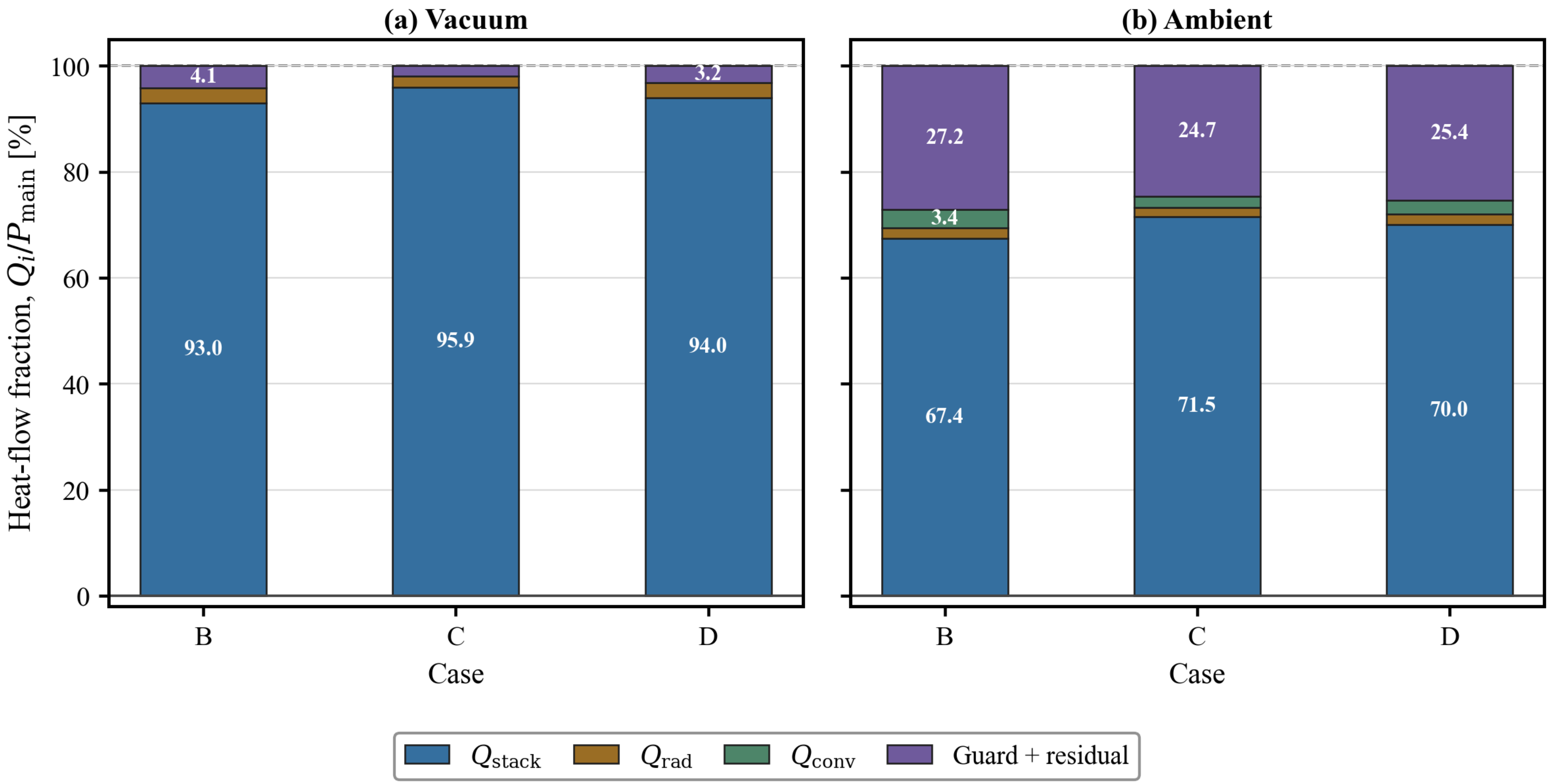

Test Article

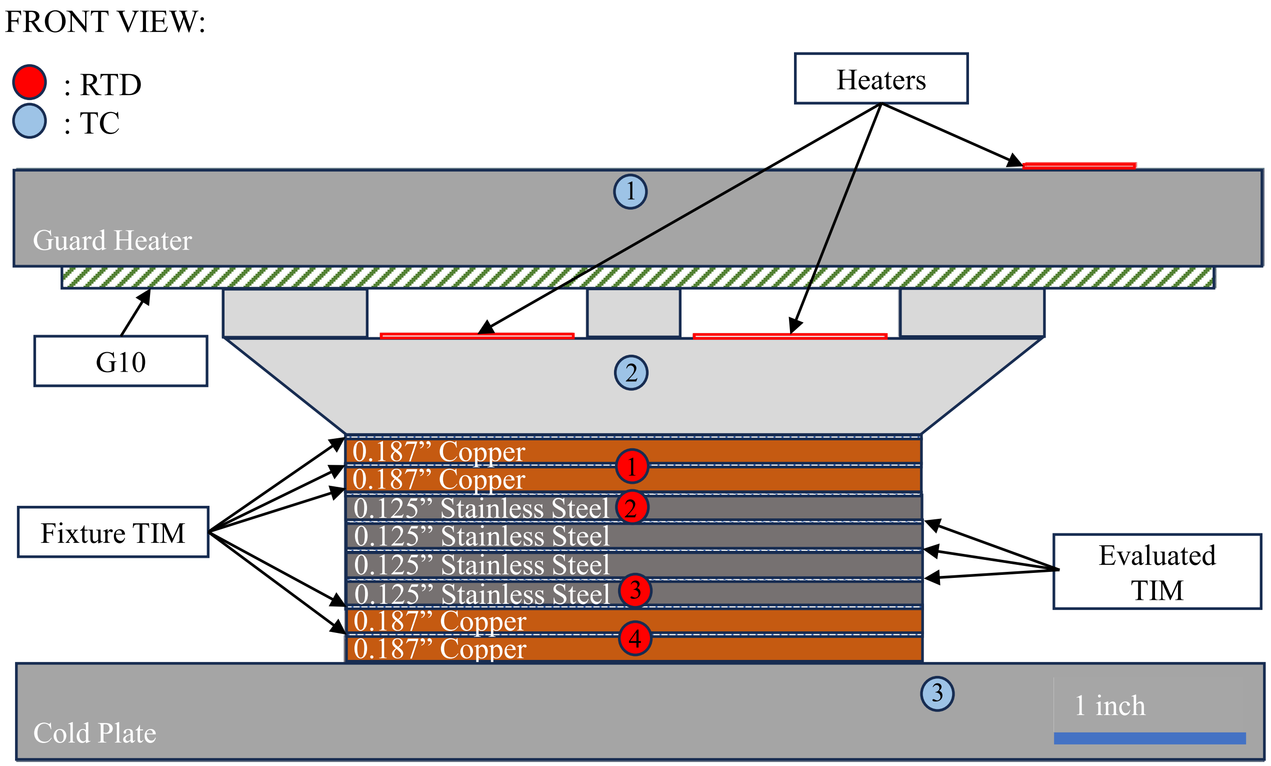

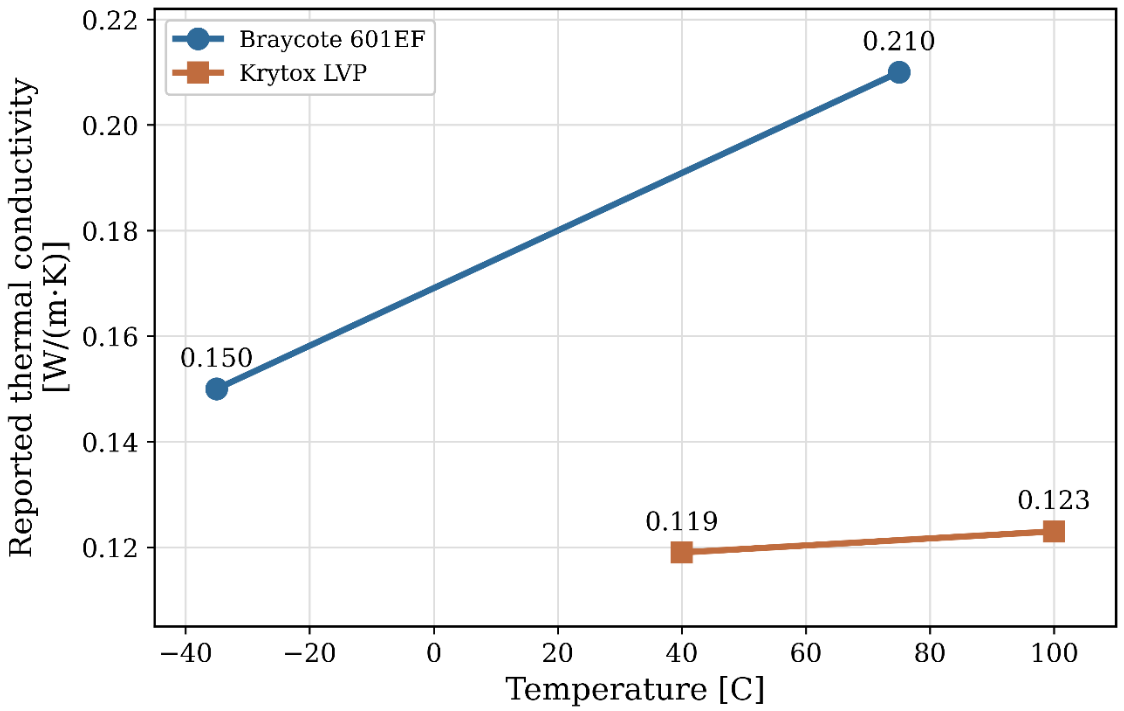

TIM	Thermal Conductivity
Braycote 601EF	0.15 W/m·K at -35ºC and 0.21 W/m·K at 75ºC
Krytox LVP	0.119 W/m·K at 40ºC and 0.123 W/m·K at 100ºC

Linear interpolation between the reported thermal conductivities is used for model validation.

[3] Castrol Industrial, 9 October 2012. [Online]. Available: https://www.2spi.com/catalog/documents/Braycote%20Micronic%20601%20EF.pdf. [Accessed June 2026].
[4] The Chemours Company, Krytox LVP Thermal Conductivity Values, 2026, Personal Communication.

Model Check: Mean Temperature Profiles

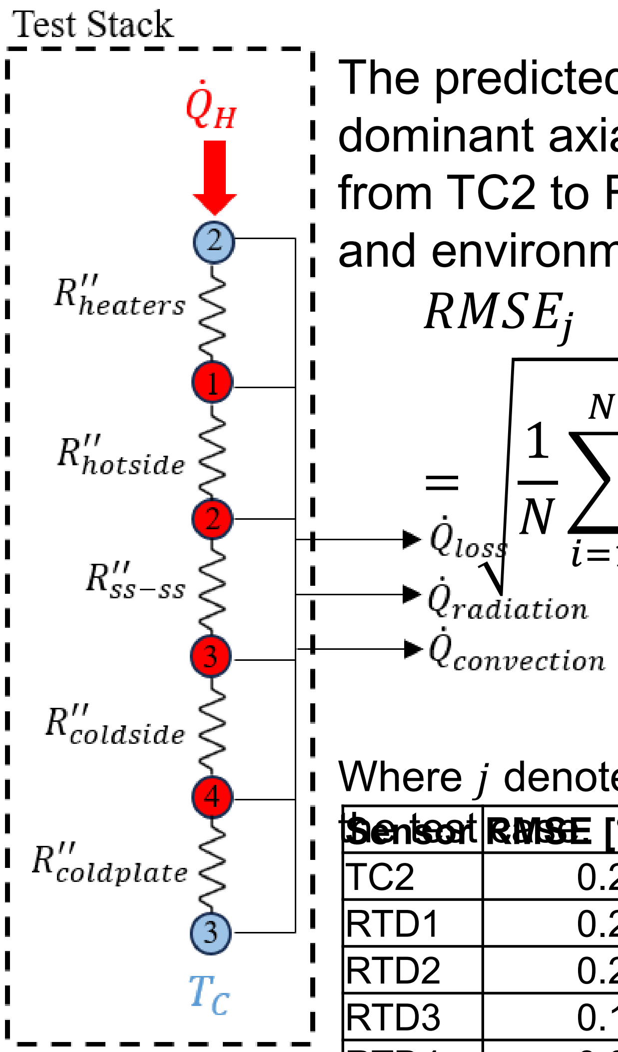

The predicted profiles capture the dominant axial temperature gradient from TC2 to RTD 4 across material and environment conditions.

$$RMSE_j = \sqrt{\frac{1}{N}\sum_{i=1}^{N}\left(T_{j,i}^{model} - T_{j,i}^{meas}\right)^2}$$

Where j denotes the sensor and i denotes the test

Sensor	RMSE [°C]	Max Abs. Residual [°C]
TC2	0.237	0.374
RTD1	0.266	0.446
RTD2	0.215	0.313
RTD3	0.179	0.291
RTD4	0.363	0.606

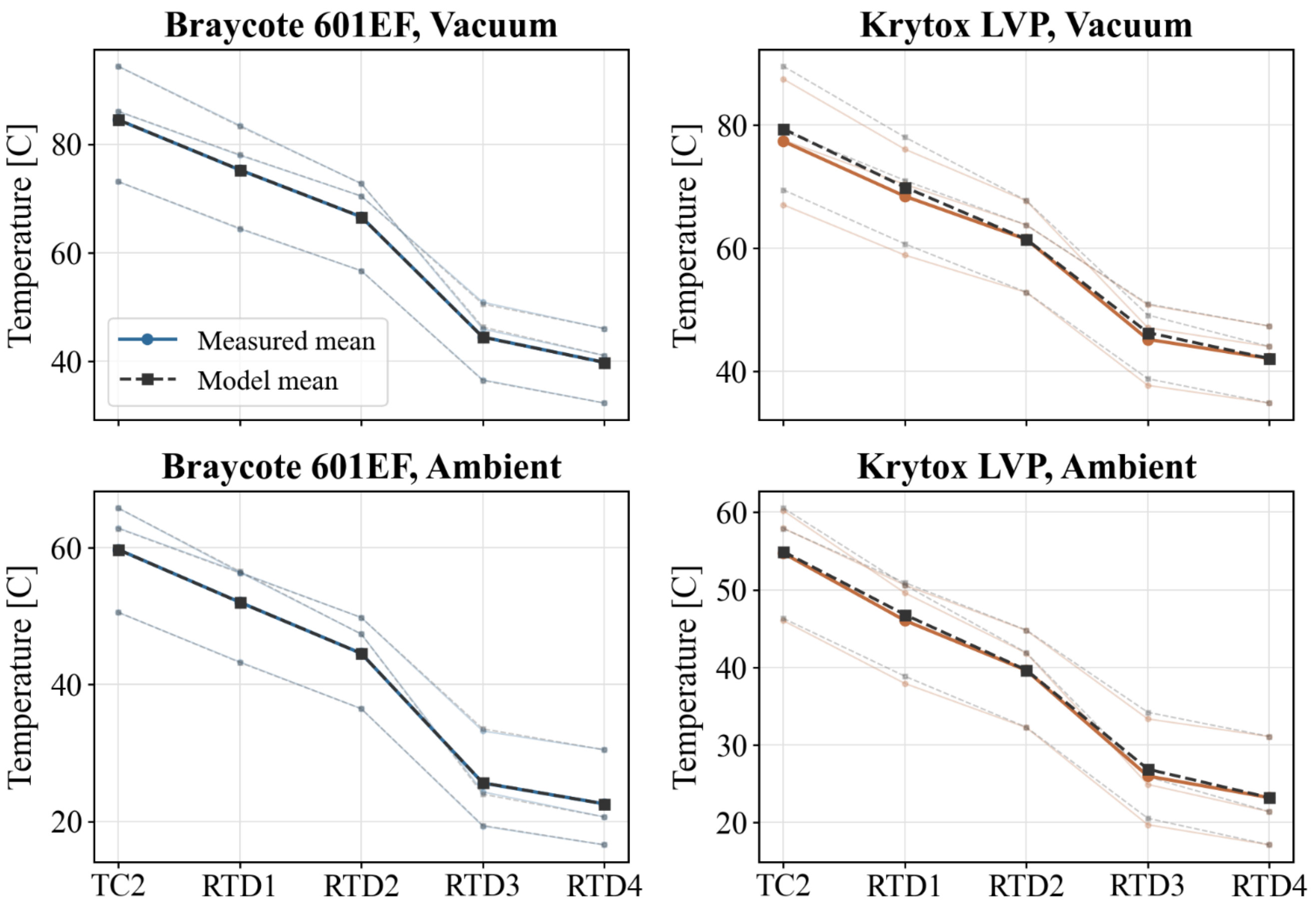

Model Check: Contact Resistances

The model derived contact resistances are physically plausible and consistent with grease-filled Cooper-Mikic-Yovanovich (CMY) rough-surface contact conductance relationship expectations, but case-to-case differences remain sensitive to inferred conductivity and are not independently measured contact changes.

Contact Resistance:

$$R''_{contact,exp} = \frac{1}{h_{asp} + h_{gap}}$$

$$h_{asp} = 1.25 k_s \left(\frac{m}{\sigma}\right)\left(\frac{P}{H_c}\right)^{0.95}, \quad h_{gap} = \frac{k_{TIM}}{Y}$$

$$k_s = \frac{2k_1k_2}{k_1 + k_2}, \qquad m = \sqrt{m_1^2 + m_2^2}$$

Roughness Separation:

$$Y = \sqrt{2}\sigma \mathrm{erfc}^{-1}\left(2\frac{P}{H_c}\right)$$

$$\sigma = \sqrt{\sigma_1^2 + \sigma_2^2}$$

Into Stack:

$$R''_{joint} = \frac{t_{TIM} - Y}{k_{TIM}} + R''_{contact,exp} + R''_{macro}$$

Where P is contact pressure, m is the mean absolute asperity slope, H_c is contact microhardness, Y is mean-plane separation, k_{TIM} is TIM thermal conductivity, and R''_{macro} is installation-scale residual resistance.

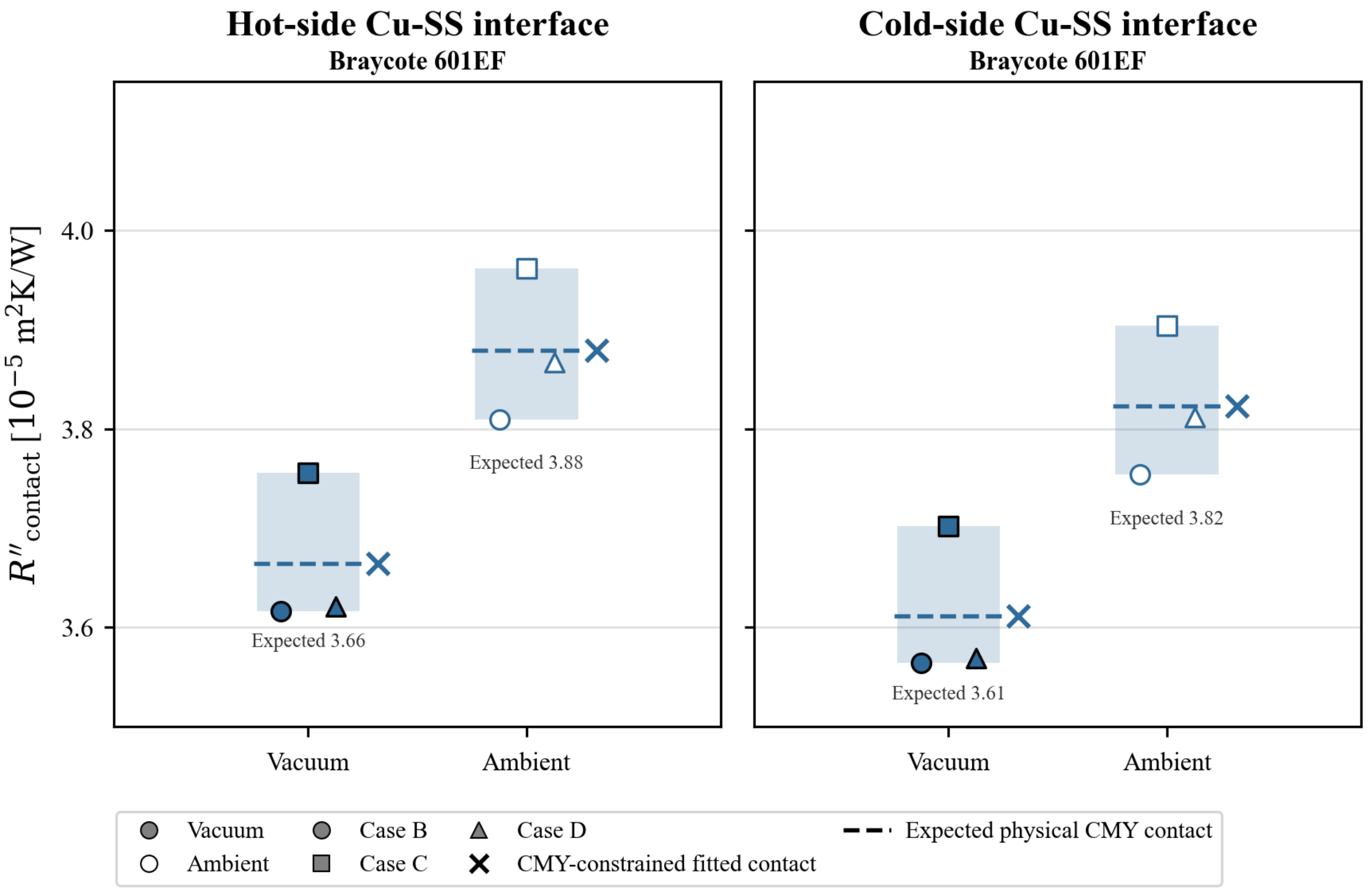

[5] Savija, I., Yovanovich, M. M., Culham, J. R., & Marotta, E. E. (2003). Thermal joint resistance of conforming rough surfaces with grease-filled interstitial gaps. *Journal of Thermophysics and Heat Transfer, 17*(2), 278–282. https://doi.org/10.2514/2.6755

Model Input Sensitivities

$$\text{sensitivity} = \text{mean}\left[\max\left(\left|k_{perturbed,-} - k_{nominal}\right|, \left|k_{perturbed,+} - k_{nominal}\right|\right)\right]$$

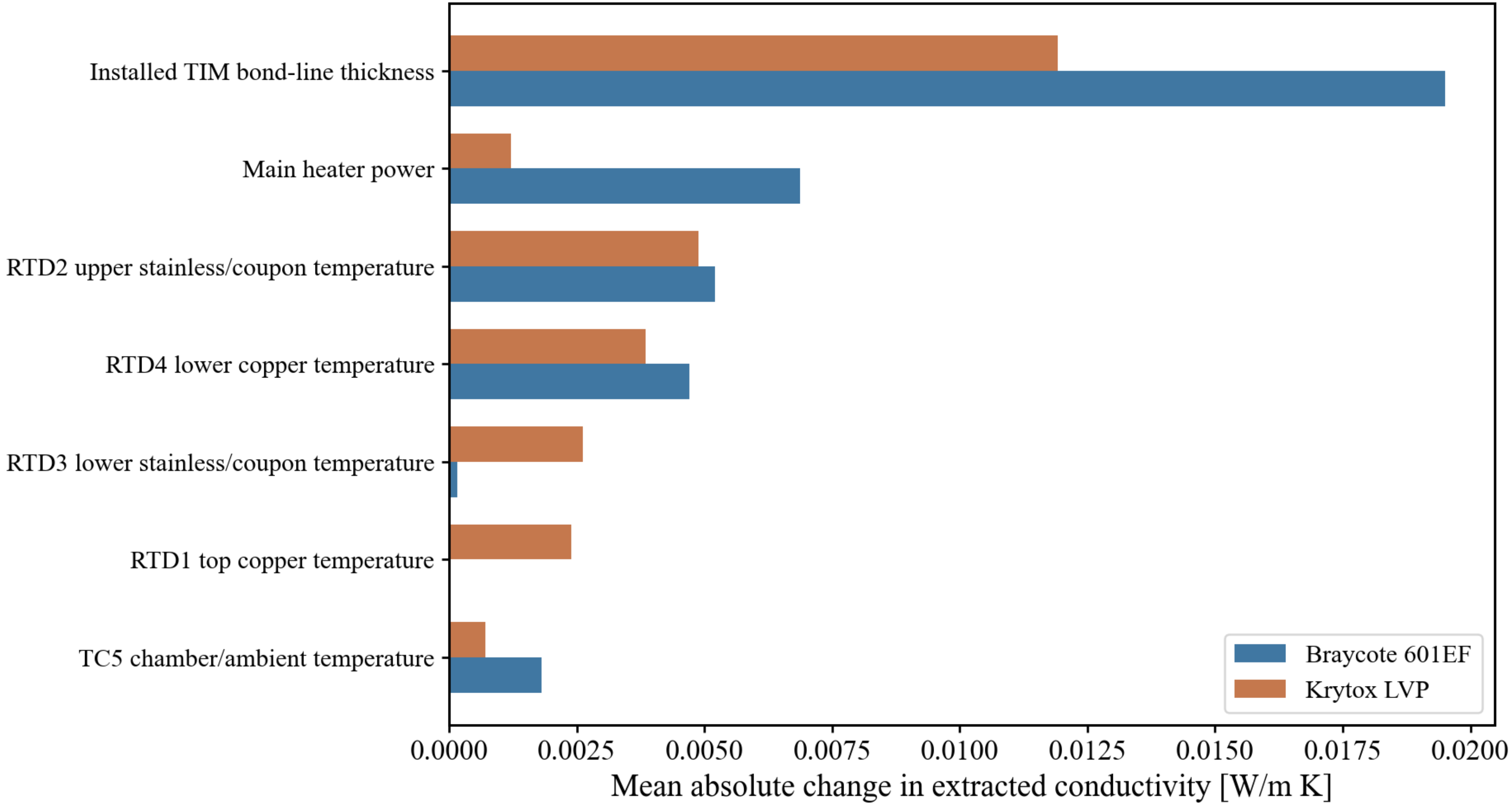

Results: Model Derived Thermal Conductivity

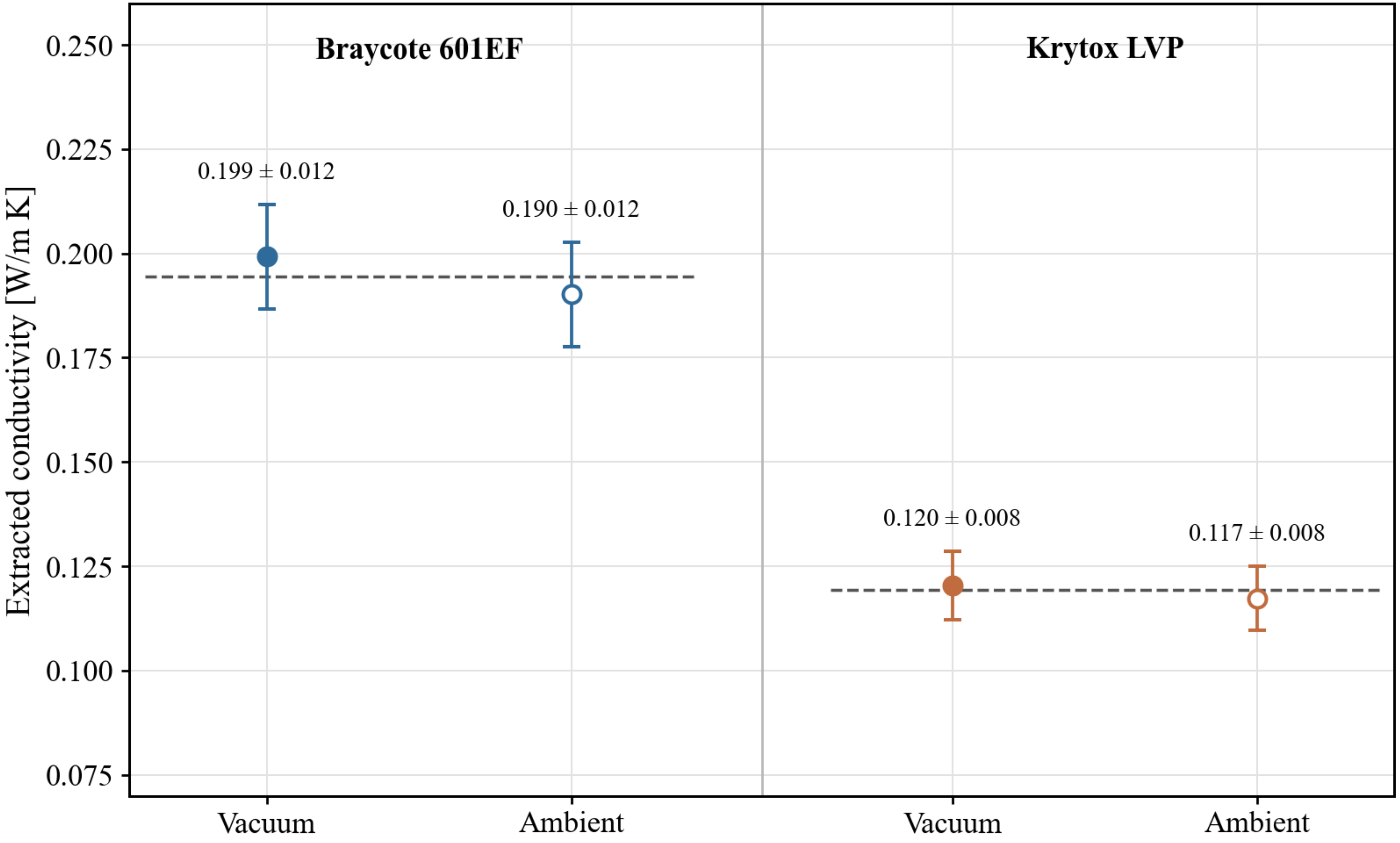

The transferred model recovers material-scale conductivity values near the reported references.

[3] Castrol Industrial, 9 October 2012. [Online]. Available: https://www.2spi.com/catalog/documents/Braycote%20Micronic%20601%20EF.pdf. [Accessed June 2026].
[4] The Chemours Company, Krytox LVP Thermal Conductivity Values, 2026, Personal Communication.

Results: Model Derived Contact Resistance

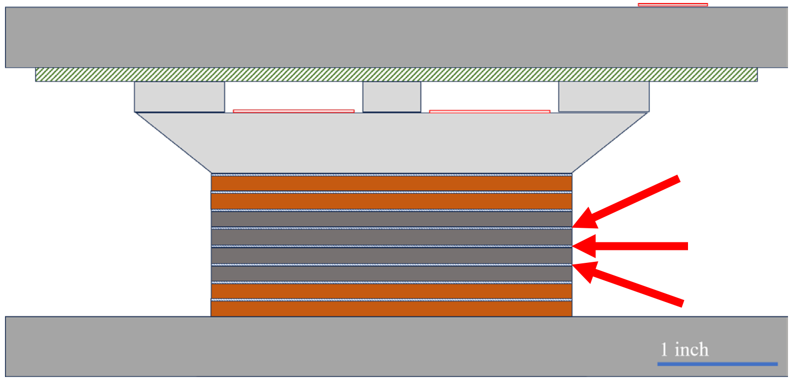

Inputs: measured surface roughness, grease $k(T)$, material properties, gravity preload.

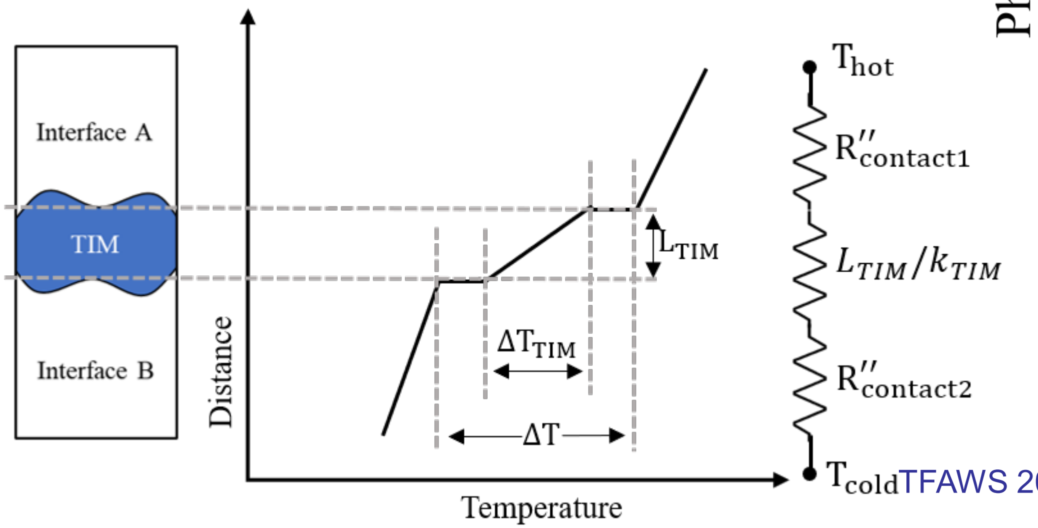

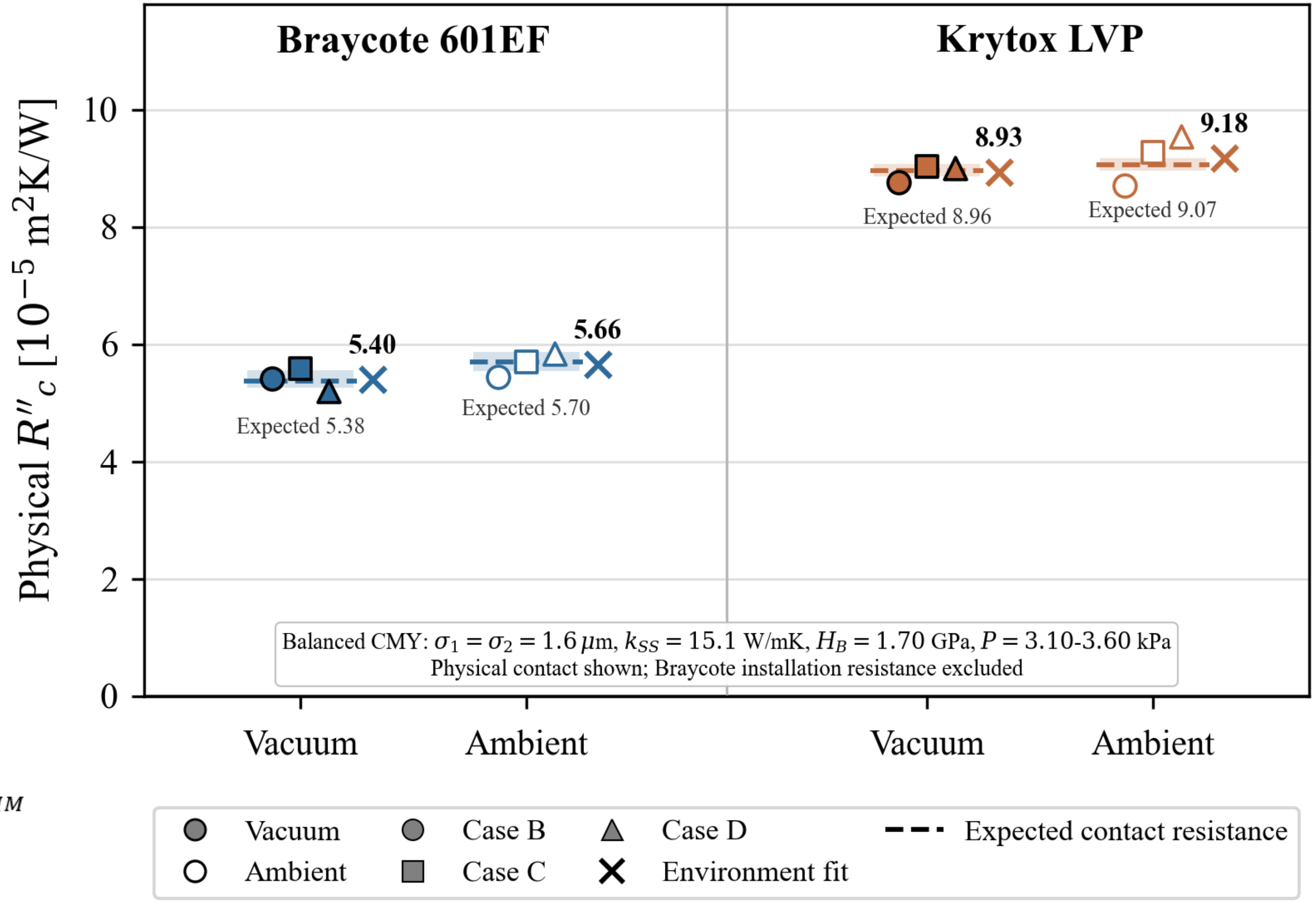

Conclusion: Spacecraft Models Need Joint Resistances

Using the model reduction, nearly a quarter of the joint resistance for Krytox was determined by contact resistances.

$$\frac{L}{k} = 3.34 \times 10^{-4}\ \mathrm{m^2K/W} \rightarrow 78.7\%$$

$$R''_{contact1+contact2} = 9.03 \times 10^{-5}\ \mathrm{m^2K/W} \rightarrow 21.3\%$$

This demonstrates the importance of understanding joint resistances, especially when designing Passive Thermal Control Systems.

Overall Impact:

- **Increased NASA MSFC Hi-TTeMP lab testing capabilities.**
- **Developed capabilities to isolate and characterize contact resistances for increased model accuracy.**
- **Increased the Technical Readiness Level (TRL) of developmental TIMs through rapid, iterative, and modular testing.**

Future Work

- Measure and control interface preload using a calibrated load cell.
- Test multiple preload and bond line thickness levels to separate material conductivity from contact resistance.
- Perform repeated assembly/disassembly trials to quantify installation repeatability.

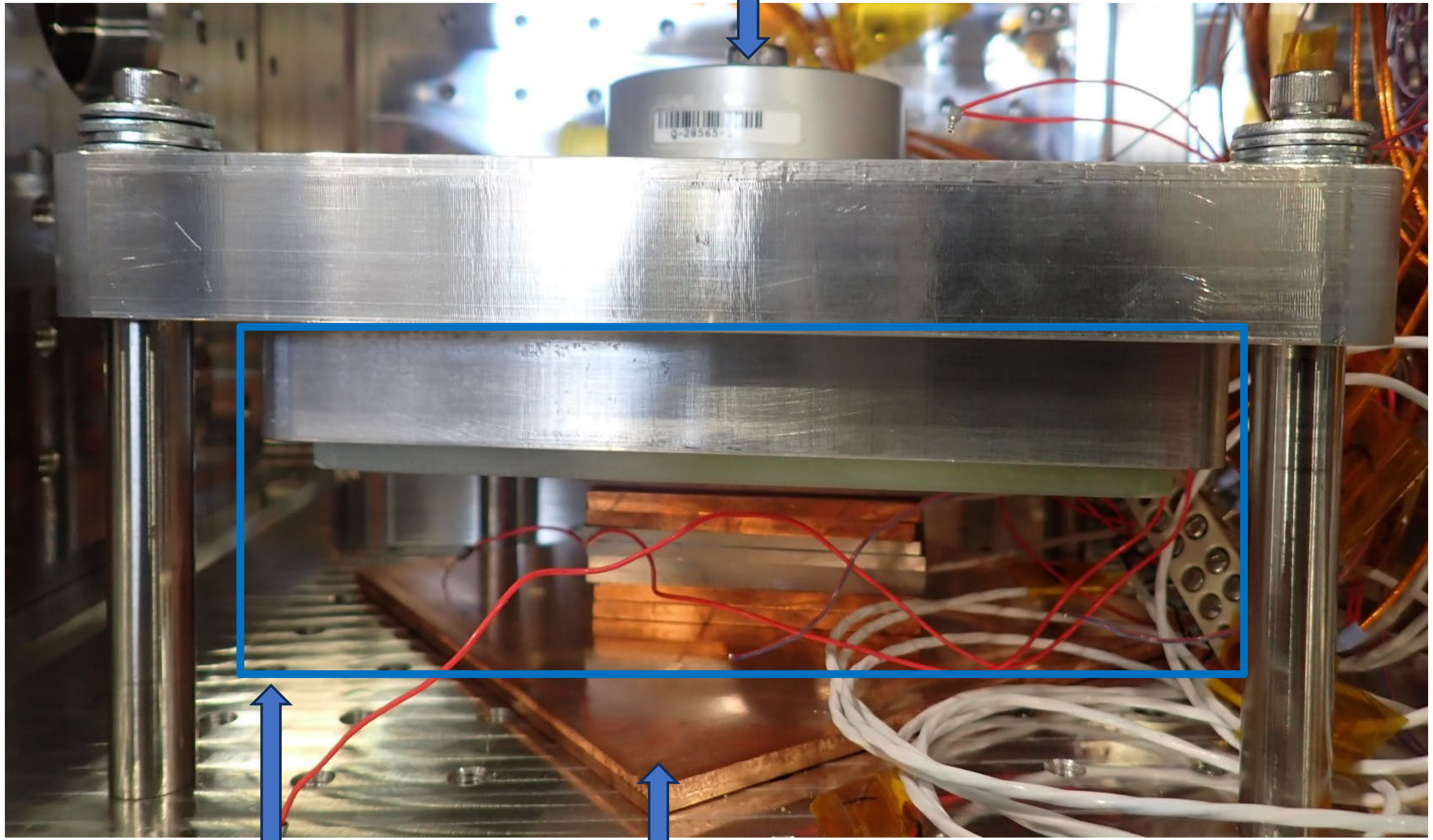

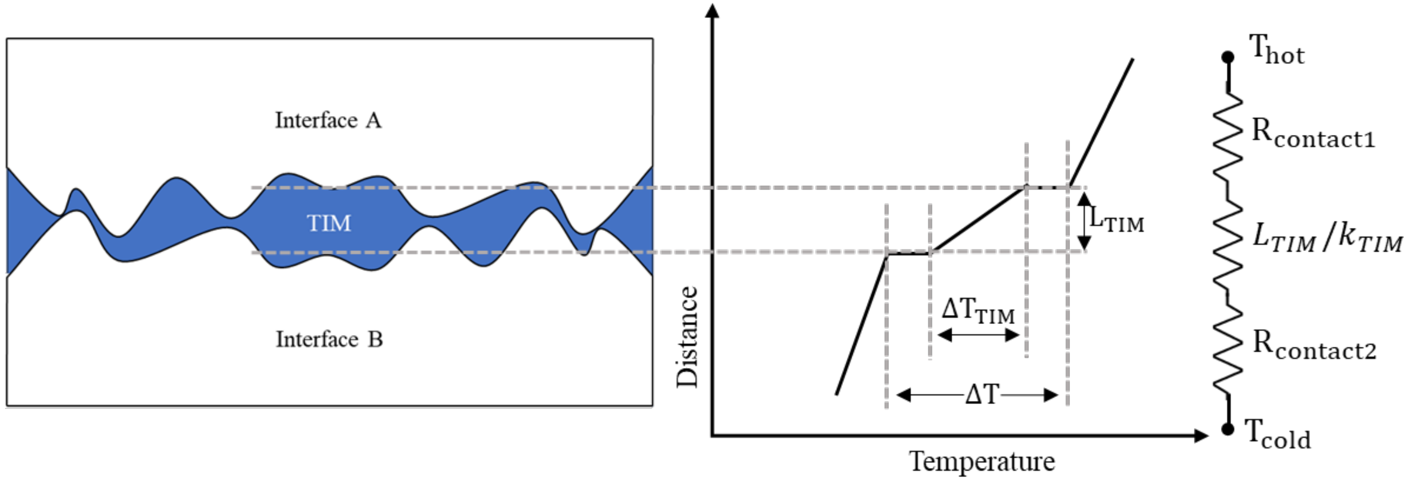

Thank you!
Questions?

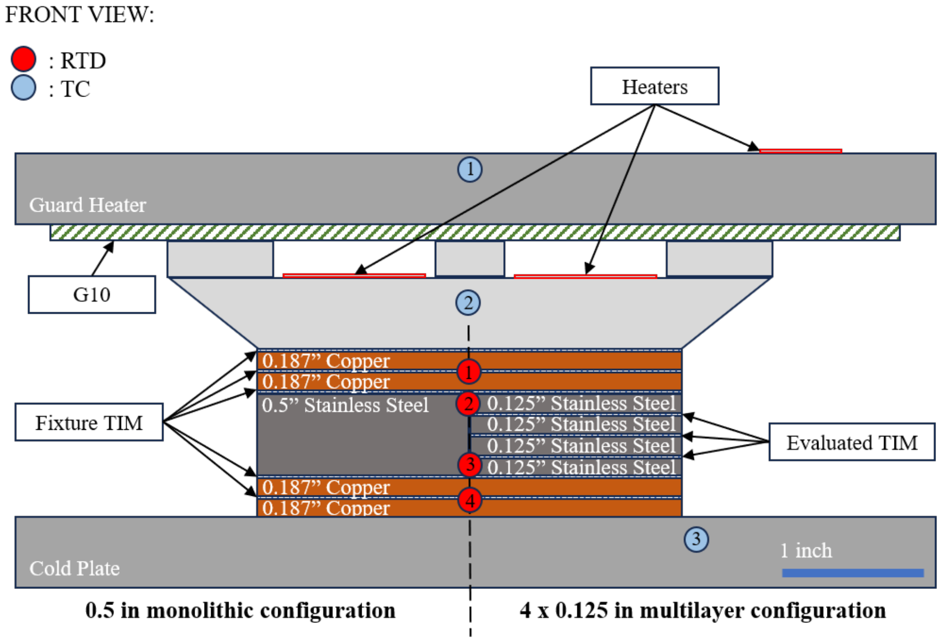

Notes:

- RTD1 and RTD4 are embedded in between the copper plates.
- TC1 was secure on the top of the guard heater.
- TC4 was secured between the MLI and the stack.
- TC5 was secured 1 inch off the vacuum chamber ceiling.

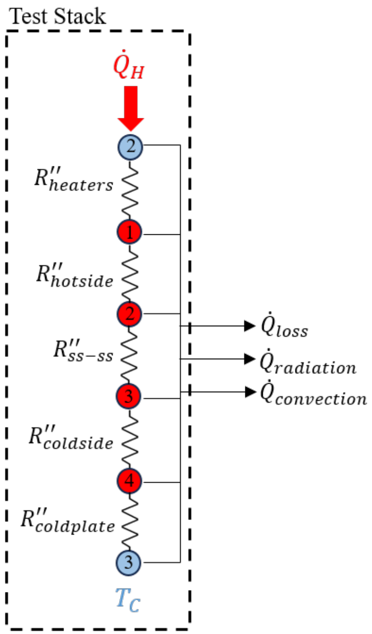

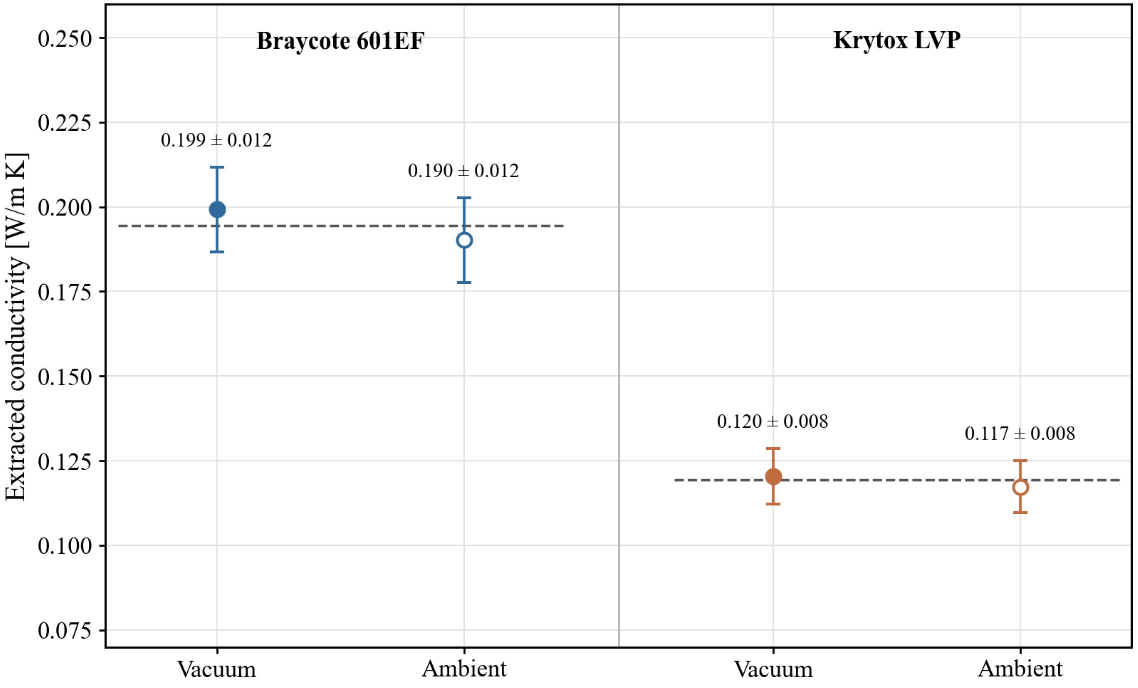

Backup Slides

Abbreviations and Acronyms

CMY	Cooper-Mikic-Yovanovich rough-surface contact conductance relationship
Hi-TTeMP	Hub for Innovative Thermal Technology Maturation and Prototyping
LVP	Low Vapor Pressure
MSFC	Marshall Space Flight Center
NASA	National Aeronautics and Space Administration
TC	Thermocouple
TIM	Thermal Interface Material
TRL	Technical Readiness Level
RMSE	Root Mean Square Error
RTD	Resistance Thermal Detector

References

[1] T. Gregory, J. Abel and J. Mandi, "Thermal Design Considerations of the Hubble Space Telescope (HST) Science Instrument Control and Data Handler (SI C&DH-2)," in 40th International Conference on Environmental Systems, Barcelona, 2012.

[2] European Space Agency, "Science Instrument Control and Data Handling Unit," 30 September 2008. [Online]. Available: https://sci.esa.int/s/8r0XPkw. [Accessed 2026].

[3] Castrol Industrial, 9 October 2012. [Online]. Available: https://www.2spi.com/catalog/documents/Braycote%20Micronic%20601%20EF.pdf. [Accessed June 2026].

[4] The Chemours Company, Krytox LVP Thermal Conductivity Values, 2026, Personal Communication.

[5] Savija, I., Yovanovich, M. M., Culham, J. R., & Marotta, E. E. (2003). Thermal joint resistance of conforming rough surfaces with grease-filled interstitial gaps. *Journal of Thermophysics and Heat Transfer, 17*(2), 278–282. https://doi.org/10.2514/2.6755

Design Criteria

Develop a modular test article that can evaluate the applied thermal conductivity of thermal interface material (TIM) in both ambient and high-vacuum environments.

- Replicate realistic aerospace-style layered thermal interfaces. → used tight tolerance components
- Characterize parasitic heat losses. → used a calibrated thermal model
- Maintain repeatable boundary conditions. → used standard heaters and cold plate
- Achieve steady-state operation. → ensured sufficient test time
- Design for controlled contact pressure testing capability. → sufficient space for load application
- Ensure compatibility with common aerospace TIMs. → used certified 304 stainless steel alloy
- Measure temperature gradients. → used Class A RTDs (±0.15°C at 0°C) and Type T TCs (±1°C)

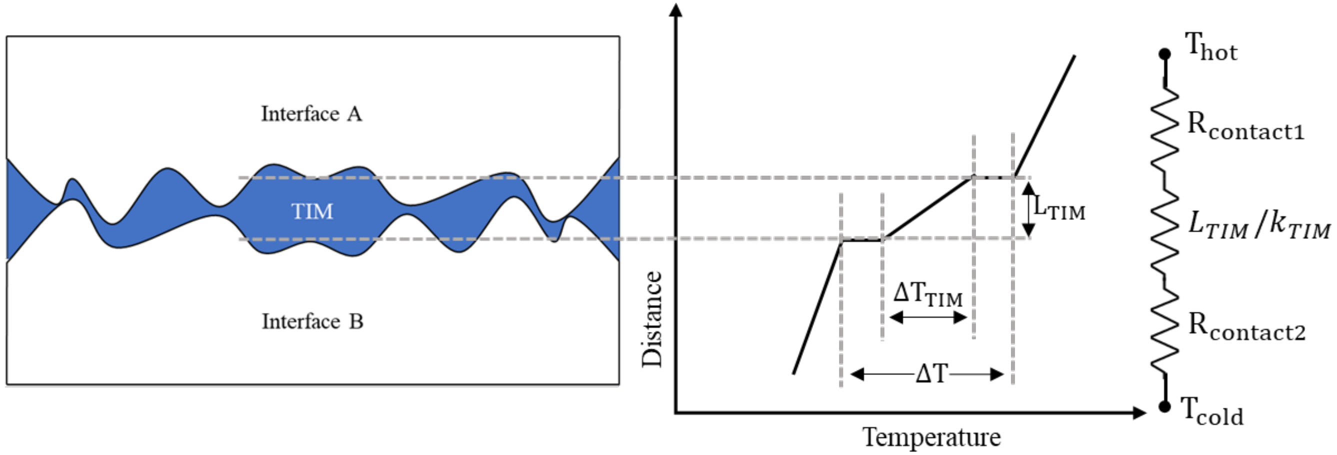

$$R''_{joint} = R''_{contact,1} + \frac{L_{TIM}}{k_{TIM}} + R''_{contact,2} = \frac{L_{TIM}}{k_{app}}$$

Experimental Configurations and Thermal Loading Conditions

Experimental Configurations

#	Configuration	Pressure	TIM	Role
1	0.5 in SS304	Vacuum	Braycote 601EF	Monolithic axial energy-consistency diagnostic
2	0.5 in SS304	Ambient	Braycote 601EF	Monolithic axial energy-consistency diagnostic
3	4 × 0.125 in SS304	Vacuum	Braycote 601EF	Four-layer calibration
4	4 × 0.125 in SS304	Ambient	Braycote 601EF	Four-layer calibration
5	4 × 0.125 in SS304	Vacuum	Krytox LVP	Validation
6	4 × 0.125 in SS304	Ambient	Krytox LVP	Validation

TIM	Thermal Conductivity
Braycote 601EF	0.15 W/m·K at -35ºC and 0.21 W/m·K at 75ºC
Krytox LVP	0.119 W/m·K at 40ºC and 0.123 W/m·K at 100ºC

Linear interpolation between the reported thermal conductivities is used for model validation.

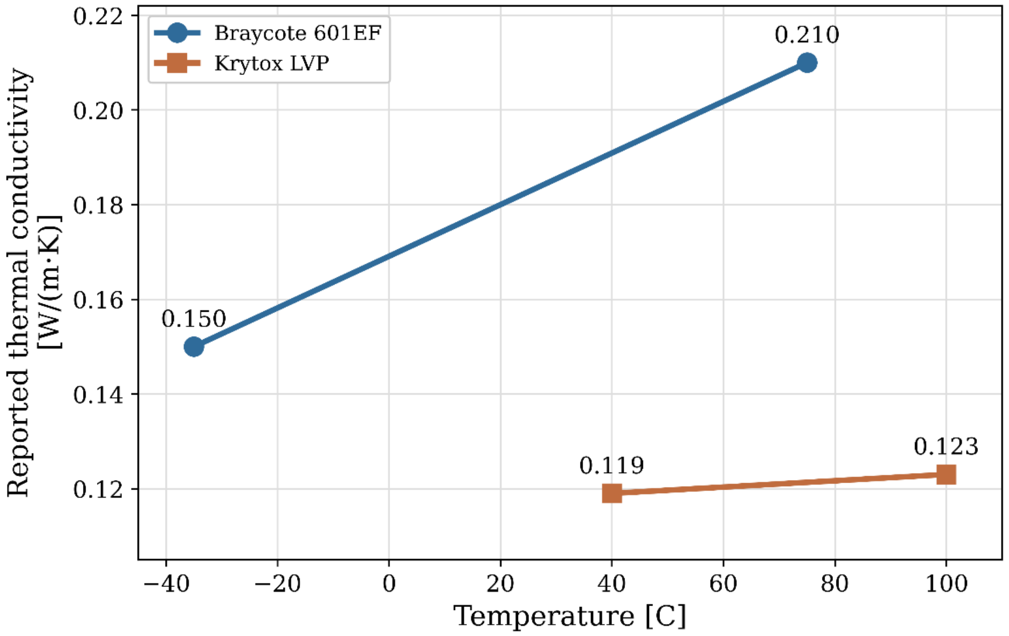

Thermal Loading Conditions

Case	Cold side setpoint [°C]	Nominal heater power [W]
A	75	20.1
B	20	45.5
C	5	45.5
D	5	62.4

[3] Castrol Industrial, 9 October 2012. [Online]. Available: https://www.2spi.com/catalog/documents/Braycote%20Micronic%20601%20EF.pdf. [Accessed June 2026].
[4] The Chemours Company, Krytox LVP Thermal Conductivity Values, 2026, Personal Communication.

Model Derived Thermal Conductivity Per Case